Hypersonic Turbulent Flow Reynolds-Averaged Navier-Stokes Simulations with Roughness and Blowing Effects

Yann Marchenay, M. Olazabal Loumé, François Chedevergne

▶ **To cite this version:**

Yann Marchenay, M. Olazabal Loumé, François Chedevergne. Hypersonic Turbulent Flow Reynolds-Averaged Navier-Stokes Simulations with Roughness and Blowing Effects. Journal of Spacecraft and Rockets, 2022, 59 (5), 10.2514/1.A35339 . hal-03740243

HAL Id: hal-03740243
https://hal.science/hal-03740243v1

Submitted on 29 Jul 2022

HAL is a multi-disciplinary open access archive for the deposit and dissemination of scientific research documents, whether they are published or not. The documents may come from teaching and research institutions in France or abroad, or from public or private research centers.

L'archive ouverte pluridisciplinaire **HAL**, est destinée au dépôt et à la diffusion de documents scientifiques de niveau recherche, publiés ou non, émanant des établissements d'enseignement et de recherche français ou étrangers, des laboratoires publics ou privés.

Hypersonic Turbulent Flow Reynolds-Averaged Navier–Stokes Simulations with Roughness and Blowing Effects

Y. Marchenay*
ONERA–The French Aerospace Lab, 31055 Toulouse, France
M. Olazabal Loumé†
French Alternative Energies and Atomic Energy Commission, 33114 Le Barp, France
and
F. Chedevergne‡
ONERA–The French Aerospace Lab, 31055 Toulouse, France

Thermal protection systems experience severe thermal load during atmospheric reentry of hypersonic vehicles. Inherent to the ablation process, roughness and blowing effects may appear, affecting the performance of the heat shield. The modeling and the simulation of these effects in the hypersonic regime are challenging and rarely compared to experimental data. In this paper, Reynolds-averaged Navier–Stokes simulations of hypersonic turbulent boundary layers with roughness and blowing wall conditions are performed on Holden's experimental configurations ("Studies of Surface Roughness and Blowing Effects on Hypersonic Turbulent Boundary Layers over Slender Cones," *27th Aerospace Sciences Meeting*, AIAA Paper 1989-0458, 1989). Using the k–ω shear stress transport model. Four experimental configurations, characterized by different levels of turbulence compressibility, are considered. A detailed discussion is proposed about the behavior of equivalent sand grain corrections and blowing corrections in combination with turbulence compressibility corrections. The predictions of skin-friction coefficients and Stanton numbers are in good agreement with Holden's experimental data. These results show that the combination of the Zeman compressibility correction and roughness/blowing wall corrections is promising for the simulation of hypersonic boundary layers over rough walls with blowing.

Nomenclature

A_p	=	roughness element projected area
A_s	=	windward surface area
C_f	=	skin-friction coefficient
F	=	blowing rate
H	=	enthalpy
k	=	turbulent kinetic energy; roughness height
k_s	=	equivalent sand grain height
l	=	averaged element spacing
M	=	Mach number
M_t	=	turbulent Mach number
P	=	pressure
Pr_t	=	turbulent Prandtl number
St	=	Stanton number
S_{corr}	=	corrected wetted surface ratio
s	=	curvilinear abscissa
T	=	temperature
u	=	streamwise mean velocity
v	=	wall-normal mean velocity
y	=	wall-normal distance
δ	=	boundary-layer thickness
ε	=	turbulent kinetic energy dissipation
ρ	=	density
ω	=	turbulent kinetic energy specific dissipation rate

Subscripts

e	=	boundary-layer edge value
w	=	wall value
∞	=	freestream value

Superscript

$+$	=	sublayer scaled value

I. Introduction

HYPERSONIC reentry vehicles see most of their surfaces become rough in the key aerothermal heating areas. On ballistic and maneuverable reentry vehicles, rough surfaces are formed by the ablation loss of the heat shield. Roughness effects on the turbulent boundary-layer flow increase heat transfer at the wall, which in return accelerates the ablation process. Simultaneously, the ablation process leads to the thermal decomposition of the materials by pyrolysis reactions. The pyrolysis products are then outgassed into the boundary layer, resulting in the blowing phenomenon. Unlike surface roughness, blowing effects on the boundary layer decrease the heat load undergone by the heat shield. Consequently, it is of critical concern for designers to be able to predict aerothermal loads in the presence of roughness and blowing effects.

Efforts were made in the 1970s and 1980s to understand the fundamental interaction between rough walls and turbulent boundary-layer flows in supersonic [1,2] and hypersonic [3] conditions. Most of the studies were dedicated to the combined effects of roughness and blowing to reproduce both effects of the transpiration-cooled and rough ablating surfaces. Few experimental studies [4–6] are available in the scientific literature to analyze pure roughness effects in hypersonic conditions. Among the available datasets, very few give access to the necessary boundary conditions for computational fluid dynamics (CFD) simulations. From this perspective, the remarkable works by Holden [3,6] are very important sources of information for CFD validation and were carefully analyzed in the present numerical study.

Received 21 December 2021; revision received 21 April 2022; accepted for publication 25 May 2022; published online 28 June 2022. Copyright © 2022 by Marchenay Y., Olazabal-Loume M., Chedevergne F. Published by the American Institute of Aeronautics and Astronautics, Inc., with permission. All requests for copying and permission to reprint should be submitted to CCC at www.copyright.com; employ the eISSN 1533-6794 to initiate your request. See also AIAA Rights and Permissions www.aiaa.org/randp.

*Ph.D. Student, Multi-Physics Department for Energetics.
†Research Scientist, Center for Scientific and Technical Study of Aquitaine
‡Research Scientist, Multi-Physics Department for Energetics.

Three main types of approaches were followed to model roughness effects in numerical simulations. Direct approaches considering resolved roughness geometries require high computational efforts and are not suitable to industrial requirements for designing reentry vehicles. Less constraining, the approach based on the discrete element method (initiated by Robertson [7] and then Finson [8]) was limited to boundary layers' codes until recent work [9]. Even though the approach is physically interesting and solidly founded, Finson's detailed numerical simulations [8] consistently overpredict the roughness-enhanced heating levels in high-speed conditions. Nonetheless, Finson's work is particularly interesting because, for his simulations, he derived roughness element specifications from profilometer traces provided by Holden [6]. These derived roughness elements can be used to provide the required parameters of roughness models. At last, the only engineering technique able to account for roughness effects in an industrial context relies on the equivalent sand grain concept. The latter dates back to the pioneer works of Nikuradse [10,11] and Schlichting [12], who explored the pressure loss increase due to sand grains in hydraulic pipe flows. From this concept, corrections applicable to Reynolds-averaged Navier–Stokes (RANS) turbulence models were derived over the years [13–15]. With this approach, correlations are used to characterize the surface through an equivalent sand grain height that, in the experiments by Nikuradse [10,11], will give the same drag increase in the fully rough regime. The equivalent sand grain height is then used as a parameter in turbulence models to artificially enhance momentum transfer at the wall, and thus reproduce the friction increase due to roughness. One of the main drawbacks of these models, which do not reproduce the physics of wall roughness, is that they preserve the Reynolds analogy and overestimate heat transfers. More recent work by Aupoix [16,17], in the framework of Menter's shear stress transport turbulence model [18], proposed a modified set of boundary conditions on walls for turbulent scalars that reproduce the friction increase due to roughness while correcting heat transfers.

Since the mid-1950s, extensive studies have been dedicated to the development of compressible turbulent boundary layers over smooth porous walls with blowing [19,20]. In most experiments, the presence of blowing leads to a strong drag and heat transfer reduction deriving from the mean wall-normal convection. In addition to skin-friction and heat transfer measurements, many authors [1,21–23] analyzed the modification of the mean velocity profile by blowing. The law of the wall in the presence of blowing is characterized by a bilogarithmic form [23] in which the integration constant decreases with the blowing velocity. In most cases, the effects of wall blowing are poorly reproduced by standard RANS models. Many RANS blowing corrections are available in the scientific literature. Most of these corrections are based on the increase of the turbulent eddy viscosity in the inner region in order to predict the correct slope of the velocity profile in the log-law region. Regarding k–ω-based turbulence models, Wilcox [24] proposed to impose the wall specific dissipation ω_w as a function of the blowing velocity. Recently, Marchenay et al. [25] derived a new correction to take blowing effects into account in the equivalent sand grain approach. This correction relies on the characterization of the velocity profile in the log-law region of turbulent boundary layers over rough walls with blowing, and it was successfully applied for subsonic and supersonic flows. The present paper is dedicated to the application of this model to hypersonic turbulent boundary layers with roughness and blowing effects.

The paper is organized as follows. The modeling strategies of roughness and the blowing effects for RANS turbulence models are presented in Sec. II. In particular, the reader is reminded of the wall corrections adapted to Menter's k–ω shear stress transport (SST) turbulence model [18] in this section. Then, Sec. III is devoted to the behavior of the k–ω SST turbulence model over Holden's hypersonic configurations [3,6]. The predicted skin friction and wall heat flux using roughness and blowing corrections are compared to Holden's experimental data.

II. Modeling

Heat transfer is a key phenomenon in hypersonic applications that must be modeled accurately, especially in presence of rough walls. For this reason, the retained turbulence model should be able to account for roughness effects on both friction and heat transfer. As mentioned earlier in this paper, the Reynolds analogy no longer holds for turbulent boundary-layer flows over rough walls. A recent turbulent model enabling the capture of dynamic and thermal effects of roughness in a RANS context is that of Aupoix [16,17]. The latter relies on the equivalent sand grain concept k_s and is built on the basis of the k–ω SST turbulent model [18]. The Aupoix roughness model was extended to blowing effects by Marchenay et al. [25], allowing the combined effects of blowing and roughness to be considered. In addition, compressible effects due to high Mach numbers must be accounted for to simulate hypersonic flows. All these model ingredients are presented thereafter in this section.

A. Compressible Turbulent Flows

The k–ω SST RANS turbulence model is widely used for engineering needs and has grown in popularity over the years. The model combines the suitability of Wilcox's k–ω model [24] to capture the near-wall turbulent flow and the k–ε model properties for free flows. A blending function F_1 ensures a continuous evolution between the two sets of coefficients. The two turbulent scalar transport equations read

$$\begin{aligned}
&\frac{\partial \rho k}{\partial t} + \frac{\partial \rho u_j k}{\partial x_j} = P_k - \beta^* \rho k \omega + \frac{\partial}{\partial x_j}\left[\rho(\nu + \sigma_k \nu_t)\frac{\partial k}{\partial x_j}\right],\\
&\frac{\partial \rho \omega}{\partial t} + \frac{\partial \rho u_j \omega}{\partial x_j} = \frac{\gamma P_k}{\nu_t} - \beta \rho \omega^2 + \frac{\partial}{\partial x_j}\left[\rho(\nu + \sigma_\omega \nu_t)\frac{\partial \omega}{\partial x_j}\right]\\
&\qquad + 2(1 - F_1)\frac{\rho \sigma_{\omega_2}}{\omega}\frac{\partial k}{\partial x_j}\frac{\partial \omega}{\partial x_j}
\end{aligned} \tag{1}$$

where $\beta^* = 0.09$, and P_k is the production term of the turbulent kinetic energy k.

Coefficients β, γ, σ_k, and σ_ω are given by the general relation for any parameter ϕ:

$$\begin{aligned}
&\phi = F_1 \phi_1 + (1 - F_1)\phi_2,\\
&F_1 = \tanh\left[\min\left(\max\left(\frac{\sqrt{k}}{\beta^* \omega y}, \frac{500\nu}{y^2 \omega}\right), \frac{4\rho \sigma_{\omega_2} k}{CD_{k\omega} y^2}\right)^4\right],\\
&CD_{k\omega} = \max\left(\frac{2\rho \sigma_{\omega_2}}{\omega}\frac{\partial k}{\partial x_j}\frac{\partial \omega}{\partial x_j}, 10^{-20}\right)
\end{aligned} \tag{2}$$

with

$$\gamma_i = \frac{\beta_i}{\beta^*} - \frac{\sigma_{\omega_i}\kappa^2}{\sqrt{\beta^*}}$$

where $\kappa = 0.41$. Table 1 notes the values of coefficients used in relation (2).

The eddy viscosity ν_t is given by the following relation:

$$\nu_t = \frac{a_1 k}{\max(a_1 \omega, SF_2)} \tag{3}$$

with $a_1 = 0.31$ and

Table 1 Coefficient values for the k–ω SST turbulence model

	β	σ_k	σ_ω
ϕ_1	0.075	0.85	0.5
ϕ_2	0.0828	1	0.856

$$F_2 = \tanh\left[\max\left(\frac{2\sqrt{k}}{\beta^*\omega y}, \frac{500\nu}{y^2\omega}\right)^2\right]$$

S is the norm of the strain tensor rate.

Associated with Eq. (1), the standard boundary conditions for smooth walls are written as

$$\begin{cases} k_w = 0, \\ \omega_w = 10\dfrac{6\nu}{\beta^*\Delta y^2} \end{cases} \tag{4}$$

where Δy is half the height of the first cell. As notably pointed out by Sarkar [26] and Zeman [27], compressibility terms related to pressure fluctuations and dilatation dissipation are neglected in order to establish the turbulent kinetic energy equation. Several reasons can be mentioned. On the one hand, there is a lack of information regarding compressibility terms for wall-bounded flows. On the other hand, the existing compressibility corrections are not widely accepted and may degrade boundary-layer predictions. Moreover, most compressibility terms are expected to be negligible, even at high Mach numbers. However, it was noted in many studies that standard RANS turbulence models tend to overpredict skin-friction coefficients and Stanton numbers for hypersonic cold-wall cases (i.e., $T_w/T_f < 1$). Therefore, the use of compressibility corrections for these configurations can significantly improve the boundary-layer predictions: in particular for Holden experiments. The review by Rumsey [28] summarized the different existing corrections applicable to the $k-\omega$ turbulence model family. The corrections derive from the compressibility terms appearing in the exact transport equation of the turbulent kinetic energy k. These terms are known as the pressure diffusion, the pressure work, the pressure–dilatation, and the dilatation dissipation terms. In turbulent boundary layers, the first two compressibility terms are presumed to be small as compared to the pressure–dilatation and the dilatation dissipation terms. The pressure–dilatation term reflects the impact of pressure fluctuations in the production and the dissipation of the turbulent kinetic energy k. Sarkar [26] proposed a pressure–dilatation correlation in the case of a homogeneous shear flow through a correction of the production and dissipation terms in the turbulent kinetic energy equation. The correction reads

$$-\alpha_1 M_t \rho P_k + \alpha_2 M_t^2 \rho\beta^* k\omega \tag{5}$$

where $\alpha_1 = 0.15$ and $\alpha_2 = 0.2$. $M_t = (\sqrt{2k}/a)$ is the turbulent Mach number, with a designating the speed of sound. The turbulent Mach number M_t represents an indicator of the compressibility of the turbulence. As suggested by Sarkar [26] and emphasized by Zhu et al. [29], this pressure–dilatation correlation is not well adapted to wall-bounded flows. However, Sarkar's correction [26] is sometimes employed for hypersonic boundary-layer simulations. The dilatation dissipation term reflects an additional dissipation caused by the compressibility of the turbulent eddies. For this reason, the dilatation dissipation term is modeled as a function of the incompressible dissipation (or solenoidal dissipation ε_s) given by the turbulence model. Sarkar et al. [30], Zeman [31], and Wilcox [32] proposed different formulations of the dilatation dissipation term ε_d based on the turbulent Mach number M_t. We retained the Zeman dilatation dissipation correction adapted to boundary layers, which reads

$$\rho\varepsilon_d = \rho\xi^* F(M_t)\varepsilon_s \tag{6}$$

$$F(M_t) = \left[1 - \exp\left(-\frac{1}{2}(\gamma+1)(M_t - M_{t0})^2/\Lambda^2\right)\right] \times H(M_t - M_{t0}) \tag{7}$$

with $\xi^* = 3/4$, $\Lambda = 0.66$, and $M_{t0} = 0.25\sqrt{2/(\gamma+1)}$. The implementation of the Zeman correction in the transport equation of the turbulent kinetic energy k yields a modification of the dissipation term as follows:

$$-\beta^*\rho k\omega[1 + \xi^* F(M_t)] \tag{8}$$

As the correction [Eq. (8)] modifies the turbulent kinetic energy k by adding an additional dissipation, the dissipation term in the ω equation must be altered as well in the following manner:

$$-\rho\omega^2[\beta - \beta^*\xi^* F(M_t)] \tag{9}$$

The implementation of the Sarkar correction [Eq. (5)] is performed in a similar way by modifying the production and the dissipation terms in the ω equation. The effect of the Zeman dilatation dissipation correction is to enhance the dissipation of the turbulent kinetic energy, and thus to decrease the turbulent shear stress in the near-wall region (high turbulent Mach number region). Consequently, this correction reduces the predicted skin-friction coefficients and Stanton numbers.

B. Roughness Effects

Nikuradse [11] showed that the outer region (i.e., the logarithmic and the wake regions) observed for boundary-layer velocity profiles over smooth walls was recovered for rough walls but shifted downward. The downward shift ΔU^+, also called the roughness function, characterizes the skin-friction coefficient C_f increase due to the presence of roughness. Indeed, letting U_e be the external boundary-layer velocity, the shift in the logarithmic region ΔU^+ imposes that

$$\Delta U^+ = U_{e_s}^+ - U_{e_r}^+ = \sqrt{\frac{\rho_e}{\rho_w}}\left(\sqrt{\frac{2}{C_{f_s}}} - \sqrt{\frac{2}{C_{f_r}}}\right) \tag{10}$$

where subscripts s and r stand for *smooth* and *rough*, respectively. Note that relation (10) only holds at the same reduced boundary-layer thickness δ^+.

From his measurements, Nikuradse [10] proposed a relation between the sand grain height k_s^+ and the roughness function ΔU^+:

$$\Delta U^+ = \frac{1}{\kappa}\ell_n\, k_s^+ + C - b_1 - b_2\,\ell_n\, k_s^+ \tag{11}$$

where $\kappa = 0.4$, and $C = 5.5$ and where

$$\begin{aligned} k_s^+ < 3.5: &\quad b_1 = 5.5, \quad b_2 = 1/\kappa, \\ 3.5 \le k_s^+ < 7: &\quad b_1 = 6.59, \quad b_2 = 1.52, \\ 7 \le k_s^+ < 14: &\quad b_1 = 9.58, \quad b_2 = 0, \\ 14 \le k_s^+ < 68: &\quad b_1 = 11.5, \quad b_2 = -0.7, \\ 68 \le k_s^+: &\quad b_1 = 8.48, \quad b_2 = 0 \end{aligned} \tag{12}$$

The subscript $+$ indicates a wall variable turned dimensionless using the viscosity ν and the friction velocity u_τ. Thus, the dimensionless sand grain height k_s^+ is defined as

$$k_s^+ = \frac{\rho_w k_s u_\tau}{\mu_w} \tag{13}$$

The relation between ΔU^+ and k_s^+ is at the core of the roughness corrections [16] developed in RANS turbulence models.

1. Friction Enhancement

The roughness correction developed by Aupoix [16] aims at reproducing the roughness function ΔU^+ observed in the logarithmic region. For that purpose, an artificial increase of the eddy viscosity ν_t at the wall is imposed, providing an increase of the turbulent contribution to the friction. It is important to note that the increase of friction due to roughness is mainly due to the pressure drag in the fully rough regime. Imposing a nonzero eddy viscosity at the wall does not respect the physics but permits us to mimic the effect of roughness on the friction coefficient.

To have nonzero values of the eddy viscosity at the wall, the boundary conditions for k and ω are modified. Expressions depending on k_s^+ were built so that for a given k_s^+, the obtained velocity shift in the logarithmic region is exactly $\Delta U^+ = f(k_s^+)$, which is prescribed by relation (11). The final boundary conditions read

$$\begin{cases} k_w^+ = \max(0, k_0^+), \\ k_0^+ = \frac{1}{\sqrt{\beta^*}} \tanh\left[\left(\frac{\ell_n \frac{k_s^+}{30}}{\ell_n 8} + 0.5\left[1 - \tanh\frac{k_s^+}{100}\right]\right)\tanh\frac{k_s^+}{75}\right], \\ \omega_w^+ = \frac{400{,}000}{k_s^{+4}}\left(\tanh\frac{10{,}000}{3k_s^{+3}}\right)^{-1} + \frac{70}{k_s^+}\left[1 - \exp\left(-\frac{k_s^+}{300}\right)\right] \end{cases} \tag{14}$$

To turn these expressions dimensional, the friction velocity u_τ and the kinematic viscosity ν are invoked:

$$\begin{cases} k_w = k_w^+ u_\tau^2, \\ \omega_w = \dfrac{\omega_w^+ u_\tau^2}{\nu} \end{cases} \tag{15}$$

This correction was validated [16,17] over a wide variety of boundary-layer flows developing over rough surfaces. However, among all the experimental data used for validation, none of them cover the hypersonic regime. Nonetheless, there is no identified limitation to the use of the roughness correction (14) for high-speed flows.

2. Heat Transfer Correction

To complete the dynamical correction presented earlier in this paper, Aupoix [17] defined an additional thermal correction in order to deviate from the Reynolds analogy. Therefore, instead of using a constant turbulent Prandtl number Pr_t to evaluate the turbulent thermal conductivity, a modified form of Pr_t was introduced by Aupoix. Three main effects are modeled with this thermal correction through three different parameters. The modification of the turbulent Prandtl number reads

$$\begin{aligned} Pr_t &= Pr_{t_s} + \Delta Pr_t, \\ \Delta Pr_t &= (A\Delta U^{+^2} + B\Delta U^+)e^{-\frac{\nu}{k}}, \\ A &= (0.0155 - 0.0035 S_{\text{corr}})[1 - e^{-12(S_{\text{corr}}-1)}], \\ B &= -0.08 + 0.25 e^{-10(S_{\text{corr}}-1)} \end{aligned} \tag{16}$$

with Pr_{t_s} as the constant turbulent Prandtl number used for smooth walls. First, the turbulent mixing enhancement due to roughness that promotes heat fluxes is accounted for through k_s^+. More precisely, the turbulent mixing increase is represented by the roughness function ΔU^+. Second, the heat transfer over rough surfaces is directly influenced by the wetted surface, i.e., the surface topology. However, in dense rough configurations, McClain et al. [33] suggested that there is a significant part of the flow around the roughness that does not contribute to heat transfer. The geometry of the roughness elements with troughs below a reference surface must be neglected. This reference surface is assumed to be the meltdown surface, i.e., the plane surface that would be obtained when the roughness is melted. For this reason, the thermal correction is parametrized with the so-called corrected wetted surface ratio S_{corr} that only accounts for the geometry of roughness above the meltdown surface. The last parameter that drives the modified Prandtl number is the mean physical height k of the rough surface. The modification to the turbulent Prandtl number must not exceed the roughness sublayer, which is generally estimated to extend up to 3–5k. Above the roughness sublayer, the velocity and temperature profiles (U^+ and T^+) are similar to those obtained on a smooth wall once scaled by the proper friction level. In other words, the turbulent Prandtl number must recover its constant value above the roughness sublayer.

C. Blowing Effects

A common way to analyze the effects of wall blowing is to characterize the mean velocity profile in the inertial region. Using the Couette flow theory, many authors [1,22,23] expressed the law of the wall for compressible turbulent boundary layers with blowing in the following form:

$$u^{**+} = \int_0^{u^+} \frac{\sqrt{\rho/\rho_w}}{\sqrt{1 + v_w^+ u^+}}\, \mathrm{d}u^+ = \frac{1}{\kappa}\ell_n\, y^+ + C(v_w^+) \tag{17}$$

with v_w as the wall-normal velocity at the wall (i.e., the blowing velocity). This form reflects the alteration of the slope of the velocity profile, which does not follow a logarithmic law in the presence of blowing. Generally, RANS turbulence models in their standard form poorly reproduce the behavior of the integration constant C, which decreases with the blowing velocity. To solve this problem, ad hoc corrections were proposed in order to enhance the turbulent eddy viscosity in the near-wall region, and thus shift the velocity profile downward. Based on Andersen et al.'s experimental work [34], Wilcox [24] modified the specific dissipation rate ω at the wall to reproduce the dependency of the integration constant C :

$$\omega_w^+ = \frac{20}{v_w^+(1 + 5v_w^+)} \tag{18}$$

One may note that Wilcox's blowing correction is similar to the roughness corrections by increasing the turbulent contribution to the skin friction.

D. Combined Effects of Roughness and Blowing

Because roughness and blowing corrections adapted to k–ω-based models impact the same wall boundary conditions, they cannot be employed simultaneously to reproduce the combined effects of roughness and blowing. Recently, Marchenay et al. [25] proposed a modification of the equivalent sand grain height k_s^+ to take blowing effects over smooth or rough walls into account. The idea of this correction is to impose the correct velocity shift ΔU^+ in the inertial region, which depends on the roughness parameter k_s^+ and the blowing parameter v_w^+. By relying on Healzer et al.'s [35], Pimenta et al.'s [36], and Voisinet's [2] experiments, Marchenay et al. [25] decomposed the velocity shift in the following manner:

$$\Delta U^+(k_s^+, v_w^+) = \Delta U_r^+(k_s^+) + \Delta U_{rb}^+(k_s^+, v_w^+) \tag{19}$$

where ΔU_r^+ is the velocity shift given by the standard roughness corrections. For all the roughness regimes, the velocity shift ΔU_{rb}^+ is expressed as

$$\Delta U_{rb}^+(k_s^+, v_w^+) = \frac{1}{\kappa}\ell_n(1 + f(k_s^+)v_w^+) \tag{20}$$

with

$$f(k_s^+) = 5.9[1 + \tanh(k_s^+ - 7)] + 4.2 \tag{21}$$

Finally, to impose the velocity shift ΔU^+, the modification of the equivalent sand grain height k_s^+ based on Nikuradse's roughness function [10,11] reads

$$k_s^+|_{\text{app}} = \max(k_1, k_2) \tag{22}$$

where

$$k_1 = k_s^+(1 + f v_w^+) \tag{23}$$

$$k_2 = \exp\left[\frac{\kappa(b_1 - C)}{1 - \kappa b_2}\right](1 + f v_w^+)^{1/(1-\kappa b_2)} \tag{24}$$

Equation (22) is included directly in the Aupoix roughness correction by modifying the equivalent sand grain height k_s^+. The correction was

detailed by Marchenay et al. [25]. The combination of the Marchenay roughness/blowing correction and the Aupoix roughness model is retained in this study to reproduce blowing effects over smooth and rough walls for hypersonic turbulent boundary layers. Furthermore, Marchenay et al. [25] proposed an extension of the Aupoix turbulent Prandtl number correction to blowing thermal effects. The roughness function ΔU_r^+ is replaced by the total velocity shift ΔU^+:

$$Pr_t = Pr_{t_s} + \Delta Pr_t\left(\Delta U^+(k_s^+, v_w^+), S_{\text{corr}}, \frac{y}{k}\right) \tag{25}$$

where the transition function f is altered in the following manner to ensure the recovery of the Reynolds analogy over smooth walls:

$$f(k_s^+) = 8[1 + \tanh(k_s^+ - 7)] \tag{26}$$

III. Boundary Layers over Rough Walls in Hypersonic Conditions

A. Holden Experiments

Holden's publications [3,5] described several experiments on rough models in the hypersonic regime. We retain four of them with a 0 deg incidence condition: a 6 deg half-angle slender cone, a 10.5 deg half-angle slender cone, a biconic model, and a hemispherical model. The studied part of the biconic model is the 45 deg half-angle cone where the roughness elements are located. These experiments were conducted in the Calspan hypersonic facility. Two freestream Mach numbers were considered in these studies. The experimental freestream conditions are summed up in Table 2. The wall temperature is fixed at 318.4 K for the 6 deg half-angle slender cone and the biconic model. According to Holden's studies, the wall-to-freestream total temperature ratio is of 0.2 at Mach 11 and 13 for the 10.5 deg half-angle slender cone and the hemispherical model. Only measurements of skin-friction coefficients and Stanton numbers are available. They are defined, respectively, by

$$C_f = \frac{\tau_w}{(1/2)\rho_\infty U_\infty^2}, \qquad S_t = \frac{\Phi_w}{\rho_\infty U_\infty (H_t - H_w)} \tag{27}$$

where H_t is the total enthalpy.

Simulations are performed using the French Alternative Energies and Atomic Energy Commission's Navier–Stokes code. This code is a structured mesh code based on a finite volume approach with a second-order total value diminishing scheme. The following simulations are performed using the k–ω SST model [18] with the Sarkar [26] or Zeman [31] compressibility correction and blowing/roughness models [25]. The flow topologies are quite simple for all the configurations. Mesh convergence was systematically checked to ensure grid independence on the distributions of both coefficients: C_f and the Stanton number St.

To perform the computations while considering the presence of roughness, turbulent flow modeling [16] requires the description of the roughness elements and their distribution. The equivalent sand grain height k_s is estimated by using different roughness correlations: those of Dirling [37], Sigal and Danberg [38], and van Rij et al. [39]. A roughness element spacing and shape parameter Λ is calculated for each correlation:

Table 2 Holden experimental conditions

M_∞	U_∞, m · s^{-1}	$T_{t,\infty}$, K	T_∞, K	$P_{t,\infty}$, Pa	P_∞, Pa
11.36	1763.5	1608	60	1.44×10^8	1450
13	1941.5	1932	55.5	1.29×10^8	520

$$\text{Dirling [37]}: \Lambda = \frac{l}{k}\left(\frac{A_s}{A_p}\right)^{4/3},$$

$$\text{Sigal and Danberg [38] and Van Rij et al.[39]}: \Lambda = \frac{l^2}{A_p}\left(\frac{A_p}{A_s}\right)^{-1.6} \tag{28}$$

where l is the averaged element spacing, A_p is the roughness element projected area, and A_s is the windward surface area. The equivalent sand grain height k_s derives directly from the estimation of the roughness parameter Λ. Table 3 sums up the estimated roughness parameters for all the configurations. The different roughness correlations lead to a moderate discrepancy between the three equivalent sand grain heights. This reflects the difficulty of estimating the equivalent sand grain height, even for uniform surface roughness elements. Because roughness effects have a logarithmic behavior in the fully rough regime, the observed discrepancy does not yield a large difference in the prediction of Stanton numbers. The recent correlation proposed by van Rij et al. [39] is adapted to three-dimensional roughness elements and provides accurate results on irregular or patterned rough surfaces. For this reason, we retained van Rij correlation in the present paper for the simulation of Holden's hypersonic configurations [3,6].

B. Hemispherical Model

Before exploring Holden's conical configurations, a hemispherical configuration is analyzed [3,40,41]. Holden [3,40,41] studied the effects of patterned conical roughness elements on hemispherical nosetips at Mach 11. The radius of the hemispherical model is 15.24 cm (6 in.). To perform the computations while considering the presence of roughness, turbulent flow modeling [16] requires the description of the roughness elements and their distribution. The retained roughness configuration is a dense arrangement of 37 conical roughness elements on a hexagonal surface of side 2.65 mm. The radius of the height and the base of the conical roughness is fixed at 0.3175 mm. The corrected wetted surface is estimated above the meltdown surface, for which the height h_m is given by

$$h_m = \frac{37\pi k^3}{3S_{\text{ref}}} = 6.8 \times 10^{-5} \text{ m} \tag{29}$$

with S_{ref} as the surface of the hexagonal surface. Finally, the corrected wetted surface ratio S_{corr} is defined by

$$S_{\text{corr}} = \frac{37\pi(k - h_m)\sqrt{2(k - h_m)^2} + S_{\text{ref}} - 37\pi(k - h_m)^2}{S_{\text{ref}}} = 1.16 \tag{30}$$

The flow topology is illustrated in Fig. 1a via the distribution of pressure around the object. Due to high temperatures in the stagnation region, ideal and nonideal gas simulations were performed using Hansen's real gas model [42]. Both simulations provide similar results. Consequently, an ideal gas assumption is used in the present simulations. Stanton numbers are presented in Fig. 1b against the curvilinear abscissa s for smooth and rough wall configurations. Over a smooth wall, experimental data are well reproduced by the simulations. Because a subsonic region is observed around the nosetip, the use of compressibility corrections is not required. For instance, the Sarkar correction (dashed–dotted–dotted lines) slightly decreases the distribution of the Stanton numbers, but only far from the stagnation point. Over a rough wall, simulations are performed without

Table 3 Equivalent sand grain height ratio

Case	Λ [37]	k_s/k [37]	Λ [38,39]	k_s/k [38]	k_s/k [39]
Hemisphere	6.48	3.99	17.92	5.69	1.97
Bicone	9.23	2.04	25.5	3.81	1.99
Cone 6 deg	5.15	6.17	11.22	8	1.94
Cone 10.5 deg	14.25	0.89	61.75	1.39	0.64

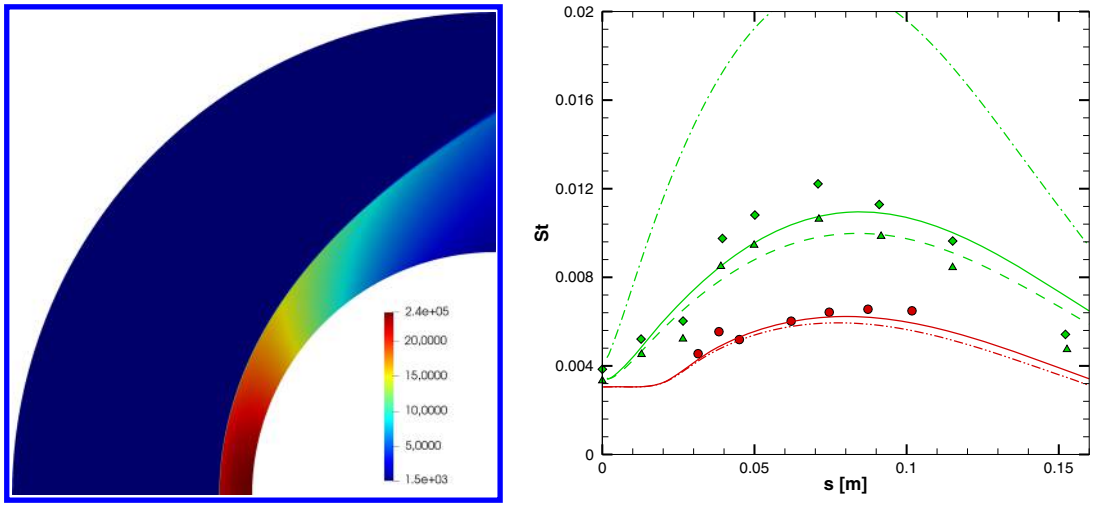

a) Pressure b) Stanton number

Fig. 1 Hemispherical model at Mach 11. Experimental data: smooth wall (circles), rough wall [3] (diamonds), and rough wall [41] (triangles). Full lines are results obtained using standard k–ω SST model with $k_s/k = 0$ or 4 (solid), with $k_s/k = 2$ (dashed), Sarkar correction with $k_s/k = 0$, and without thermal roughness correction [Eq. (16); $k_s/k = 4$] (dashed–dotted).

compressibility corrections. Two sets of experimental data relating to the same configuration are available and provide an idea of the scattering of Holden's data [3,41]. The use of the Dirling correlation $k_s/k = 4$ (solid lines) or the van Rij correlation $k_s/k = 2$ (dashed lines) to estimate the equivalent sand grain height yields very good predictions of Stanton numbers along the hemisphere. At maximum heat transfer ($s \approx 0.08$ m), the roughness Reynolds number k_s^+ is around 1000. The difference between Holden's data (diamonds) and the simulation ($k_s/k = 4$) is around 13% at this position. Because roughness effects follow a logarithmic behavior in the fully rough regime, the Dirling correlation and the van Rij correlation lead to similar results at this high roughness Reynolds number. Moreover, given the high measurement uncertainties, both correlations seem efficient. Using the Sigal and Danberg correlation, Stanton numbers are close to those predicted by the Dirling correlation. Without thermal corrections [Eq. (16); dashed–dotted lines], the Stanton numbers are significantly overestimated, which reflect the loss of the Reynolds analogy for turbulent boundary layers over rough surfaces. One may note that the Stanton numbers over a rough wall are well recovered in the stagnation region. Nevertheless, by nature, the equivalent sand grain approach is not adapted to stagnation point flows because the streamlines are no longer parallel to the rough surface. Therefore, its application may lead to poor predictions of the wall heat flux close to the stagnation point.

C. Bicone

In the experiment conducted with a biconic model, only the 45 deg half-angle conical part is of interest. Stanton number measurements are available on the smooth and rough wall cases. Simulations give a boundary-layer edge with $M_e = 1.8$ and $T_e = 940$ K. Distributions of the Stanton number St are shown in Fig. 2. The laminar–turbulent transition is imposed at $s = 4.3$ cm by a brutal switch on the production term of the turbulent kinetic energy. The simulation of the laminar upstream flow and turbulent downstream flow over a smooth wall is in good agreement with the experimental data. Because turbulent Mach numbers are low for this configuration, the Sarkar compressibility correction induces a weak effect on Stanton numbers while the Zeman compressibility correction is not activated.

From an analysis of profilometer measurements, Finson [8] proposed a geometrical definition of the representative roughness for several supersonic/hypersonic configurations: among which, the present experiment by Holden [6] is considered. It is referenced as the "4 mils" height element (1 mil $= 2.54 \times 10^{-2}$ mm). The estimated equivalent sand grain height k_s is given in Table 3. The corresponding parameters in the simulations are $k_s = 2.03 \times 10^{-1}$ mm using the van Rij et al. correlation [39] and $S_{\text{corr}} = 1.11$. The

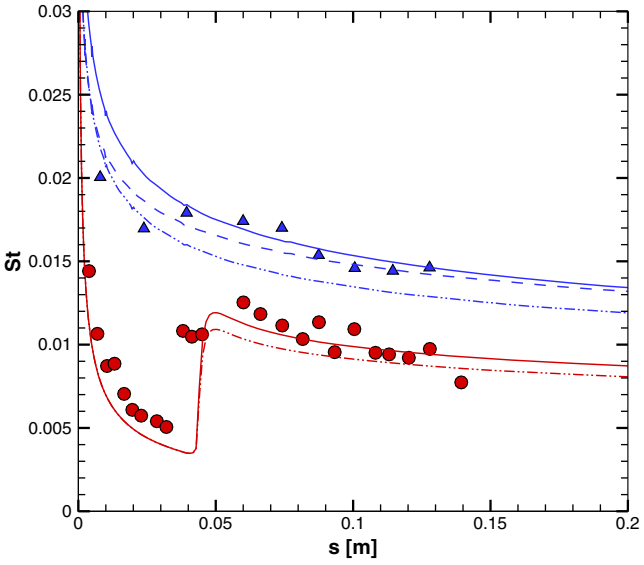

Fig. 2 Stanton number St distributions for smooth and rough cases of biconic configuration at Mach 11: smooth wall (circles), and rough wall (triangles). Full lines are results obtained using k–ω SST model without compressibility corrections (solid), with Zeman correction (dashed), with Sarkar correction (dashed–dotted–dotted).

simulations are in very good agreement with the experimental data, confirming the ability of the roughness modeling [Eqs. (14) and (16)] to evaluate turbulent flows on rough walls in the hypersonic regime. In the present case, the modification of the turbulent Pr_t number [Eq. (16)] plays a decisive role in recovering the Stanton number increase due to roughness effects. Without compressibility corrections, the roughness Reynolds number k_s^+ is close to 600 at the end of the cone. Note that by using the Sarkar correction, the Stanton number is slightly underestimated as compared to the Zeman correction or the standard $k - \omega$ SST model. The difference rises up to around 14% at the end of the 45 deg conical part.

D. Six-Degree Slender Cone

A laminar–turbulent transition was indicated by Holden [6] in the case of a smooth wall only, which was related to a junction between the elements and located 5 in. downstream of the forward tip. The origin of the curvilinear abscissa s is taken from this location. To avoid laminar–turbulent transition issues, simulations are performed by considering a fully turbulent flow. This assumption does not raise

significant differences because the majority of the experimental data is taken far from the nosetip.

Again, on rough walls, the analysis by Finson [8] provided an averaged rough element referred as the "10 mils" height element. Different correlations may be used to calculate the equivalent sand grain k_s (see Table 3). The van Rij et al. correlation, which is well suited for three-dimensional roughness configurations, is adopted here. Using the van Rij correlation with the roughness description given by Finson [8], the equivalent sand grain is found to be $k_s = 4.93 \times 10^{-1}$ mm, whereas the corrected wetted surface ratio is $S_{\text{corr}} = 1.17$.

Skin-friction coefficients and Stanton numbers are shown, respectively, in Figs. 3a and 3b. Experimental data are compared to simulations with or without compressibility corrections. From the simulations, the boundary-layer edge conditions correspond to $M_e = 9.25$ and $T_e = 88$ K. Regarding skin-friction predictions over a smooth wall, the simulations are in good agreement with the Holden experiments using the Zeman or Sarkar compressibility corrections. Without corrections, the skin-friction coefficients are clearly overestimated, which illustrates the limitations of the standard k–ω SST turbulence model in the hypersonic regime. Conversely, the interest of compressibility corrections on Stanton number predictions is not obvious because Stanton numbers are slightly underestimated using the Zeman or Sarkar corrections. Furthermore, one may note that the Zeman and Sarkar corrections are equivalent for the smooth wall case, whereas their foundations are different. Simulations using the Aupoix roughness corrections recover the increase of C_f and the Stanton number St due to roughness effects. Without compressibility corrections, the roughness Reynolds number k_s^+ is close to 120 at the end of the cone. With the Sarkar or Zeman corrections, the roughness Reynolds number is slightly reduced but remains in the fully rough regime. A reasonable agreement is found between the experimental data and the simulation results using the Zeman correction. The skin-friction coefficients C_f seem overestimated by simulations with the Sarkar correction or without compressibility corrections. However, the validity of the Stanton number predictions is not clear because the global shape of the Stanton number distribution is more pronounced in the experiment. Indeed, the experimental data reach a level as low as the one obtained on the smooth wall.

We remark that complementary simulations accounting for a laminar–turbulent transition in the rough configuration provide very similar results, indicating that the observed discrepancies are not related to the existence of a possible transition. It is suspected that compressible near-wall interactions between the roughness and the boundary layer are responsible for the observation. Indeed, the external boundary-layer velocity is such that $M_e = 9.25$, and the flow near the roughness crest may remain supersonic. Equation (11), relating ΔU^+ and k_s^+, does not include compressibility effects because it is derived from incompressible experiments. In other words, a variable k_s^+ could help in recovering the observed trend in Fig. 3. Unfortunately, there is neither experimental data nor any computation able to provide further information on this point.

E. 10.5-Degree Slender Cone

Holden et al. [3,43,44] conducted a series of three experimental studies of separate and combined effects of surface roughness and blowing in hypersonic turbulent boundary layers over a 10.5 deg sharp slender cone. Natural laminar–turbulent transition occurred within 15 cm of the nosetip (15% of the model length). Measurements obtained along the cone surface are skin-friction coefficients and Stanton numbers using a shear stress balance and calorimeter gauges. The range of the blowing coefficients of $B_h = F/St_0$ varied from zero to five in all experiments using nitrogen injectant. The blowing rate F is defined as

$$F = \frac{\rho_w v_w}{\rho_e u_e} \tag{31}$$

The first investigation was concerned with the combined effects of surface roughness and blowing. Patterned hemispherical roughness elements were used in this experiment. However, only a little information is available in Holden's report [3]. Based on the model geometry, we estimate the roughness height k at 1.2 mm. The wetted corrected surface ratio is calculated in view of the roughness density:

$$S_{\text{corr}} = 1 + \frac{2\pi k^2}{l^2} \approx 1.1 \tag{32}$$

where l is the calorimeter gauge side (i.e., the spacing between roughness elements). As noted previously, the different roughness correlations are used to calculate the equivalent sand grain k_s (see Table 3). A value of 0.77 mm is considered for the equivalent sand grain height according to the roughness correction of van Rij et al. [39]. The second experiment provides heat transfer and skin-friction measurements on a transpired turbulent boundary layer without roughness effects. The effects of the molecular weight and specific heat of the cooling injectant were studied in the last experiment but are not discussed in the present paper. In 2008 and 2011, Holden et al. [41,45] reviewed their experiments and provided some additional information and analyses.

First, we consider the smooth wall configuration without blowing conditions at Mach 11 and Mach 13. The skin-friction coefficients

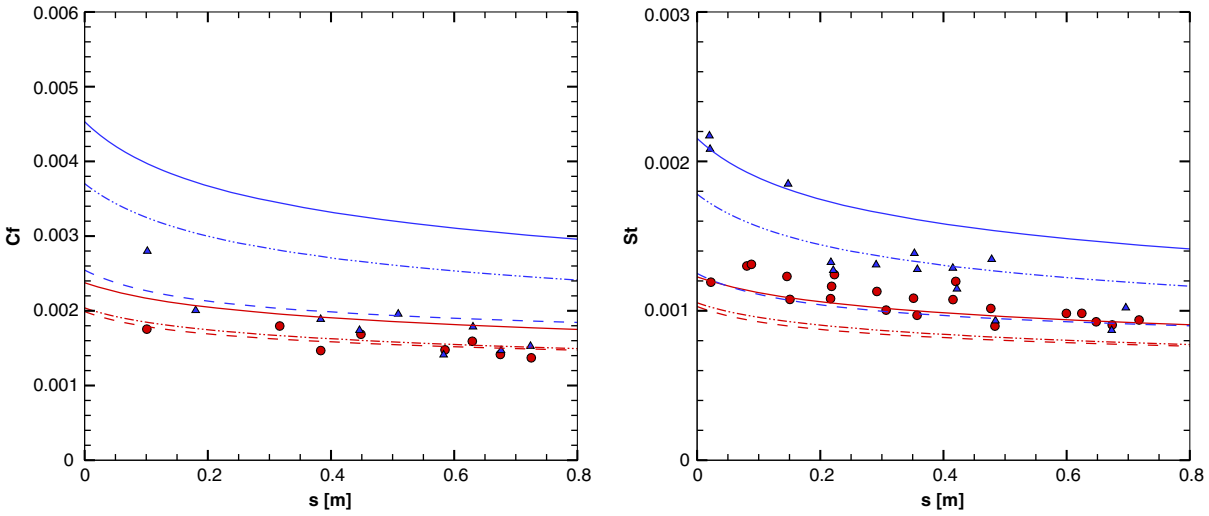

a) Skin-friction coefficient b) Stanton number

Fig. 3 Distributions of skin-friction coefficients C_f and Stanton numbers St for slender cone at Mach 11: smooth wall (circles), and rough wall (triangles). Full lines are results obtained using k–ω SST model without compressibility corrections (solid), with Zeman correction (dashed), and with Sarkar correction (dashed–dotted–dotted).

and Stanton numbers along the cone are presented in Fig. 4. The ratio s/c represents the curvilinear abscissa s scaled by the total length of the cone c. Without compressibility corrections (solid lines), the skin-friction coefficients and Stanton numbers are overestimated at Mach 11 and are well reproduced at Mach 13. At Mach 11, the difference rises up to about 35% for the skin-friction coefficient and 20% for the Stanton number at the end of the cone. There is no obvious reason that explains this result because the effects of the

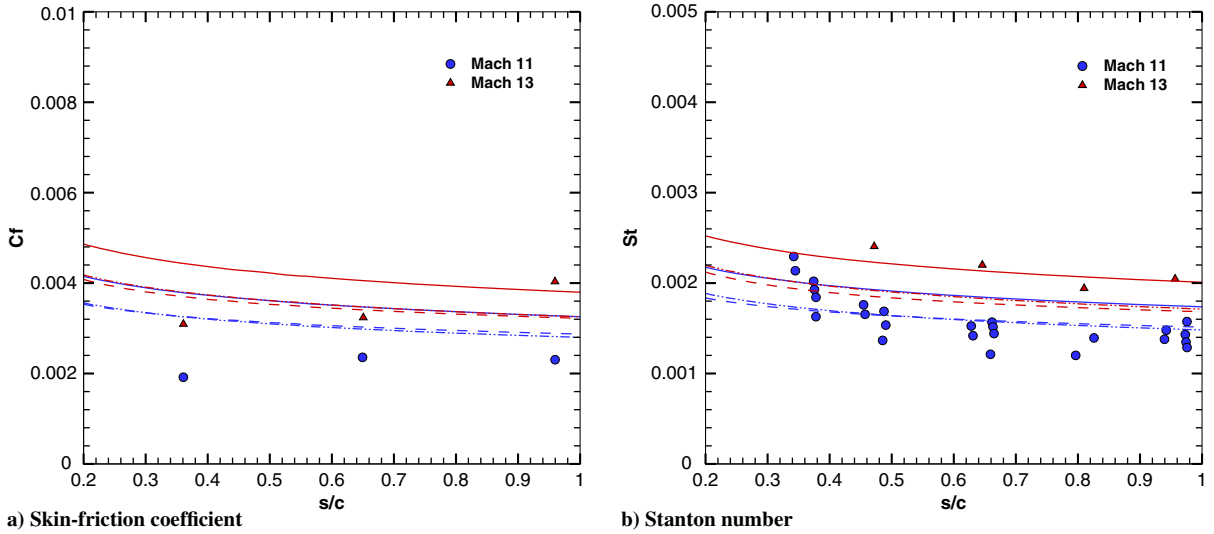

a) Skin-friction coefficient b) Stanton number

Fig. 4 Distributions of skin-friction coefficients C_f and Stanton numbers St. Full lines are results obtained using k–ω SST model without compressibility corrections (solid), with Zeman correction (dashed), and with Sarkar correction (dashed–dotted–dotted).

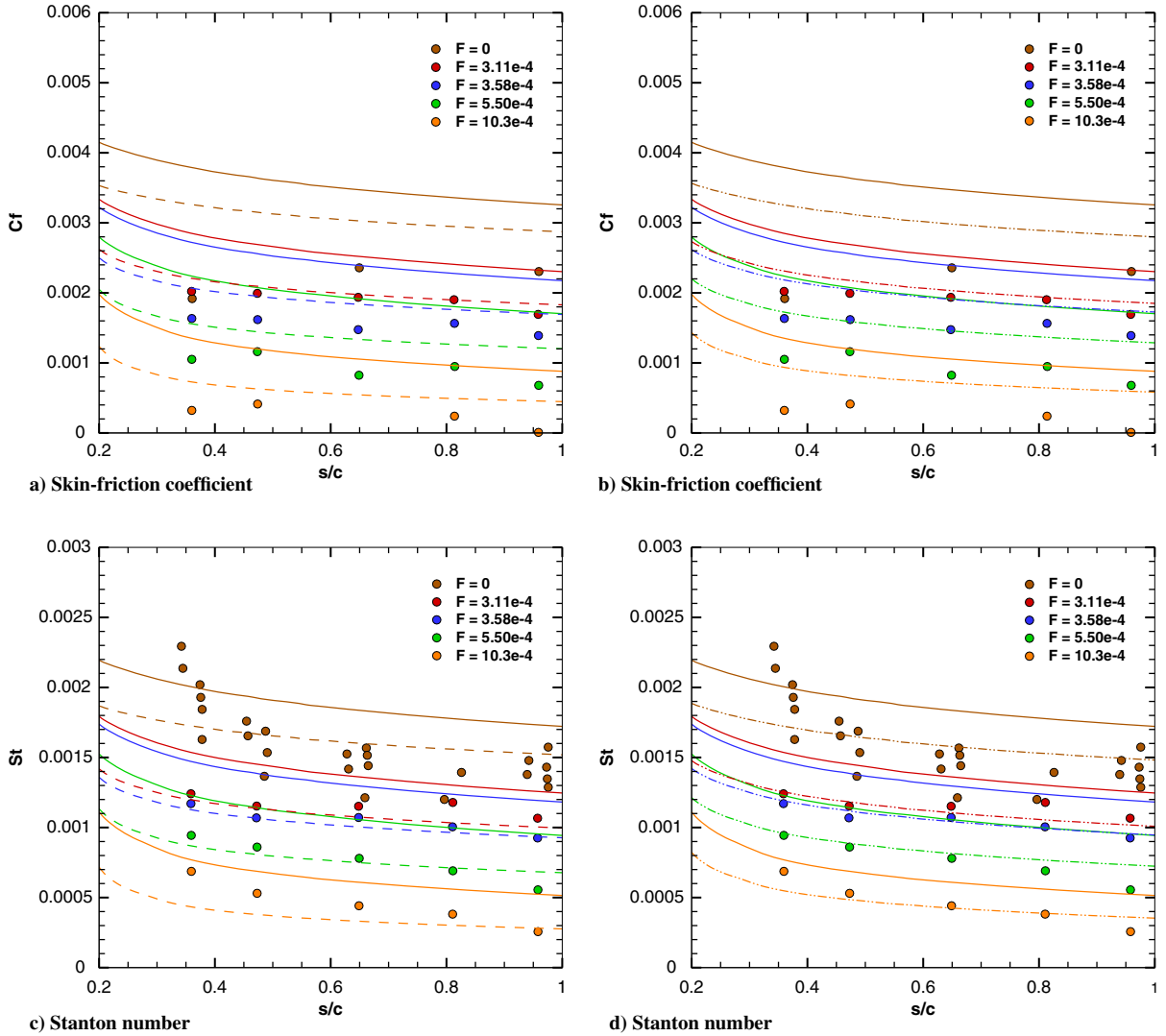

a) Skin-friction coefficient b) Skin-friction coefficient

c) Stanton number d) Stanton number

Fig. 5 Distributions of skin-friction coefficients C_f and Stanton numbers St for several blowing rates F at Mach 11. Full lines are results obtained using $k-\omega$ SST model without compressibility corrections (solid), with Zeman correction (dashed), and with Sarkar correction (dashed–dotted–dotted).

turbulence compressibility are expected to be higher at Mach 13. With the Zeman or Sarkar corrections, the predictions are in very good agreement with the experimental data at Mach 11. One may note that both compressibility corrections provide similar results. In view of the experimental data behavior at Mach 13, the reliability of these measurements is questionable. The next configuration concerns the effects of blowing over a smooth wall at Mach 11. The distribution of the skin-friction coefficients and Stanton numbers along the cone for several blowing rates F is illustrated in Fig. 5. To take the blowing effects into account in the k–ω SST model, simulations were performed using blowing/roughness corrections [Eqs. (22) and (25)] with a zero equivalent sand grain height k_s. The Sarkar and Zeman corrections improve boundary-layer predictions by decreasing the Stanton numbers and skin-friction coefficients. The behavior of the Stanton numbers is well recovered for all blowing configurations, proving the efficiency of this strategy. Without compressibility corrections, the k–ω SST model largely overestimates the skin-friction coefficients and Stanton numbers. For instance, the Stanton numbers are overestimated by 60% for the blowing rate of $F = 5.5 \times 10^{-4}$ at the end of the cone. Note that Holden's [3] measurements of skin friction are generally lower than numerical predictions, regardless of the corrections used and the configurations considered. However, in view of the experimental uncertainties over the skin-friction measurements, the combination of a wall blowing correction and a compressibility correction is a satisfying choice for hypersonic configurations over a smooth wall with blowing.

The last configuration concerned the combined effects of roughness and blowing at Mach 11 and Mach 13. The distributions of the Stanton numbers for both Mach numbers are presented in Fig. 6. The numerical comparison is performed on the predictions of the combined roughness/blowing correction and the standard roughness correction in association with the Zeman compressibility correction. Simulations using the Sarkar compressibility correction or the standard k–ω SST model were carried out but led to a large overestimate of the wall heat transfer. In fact, the combination of a roughness correction and a compressibility correction is very sensitive because roughness corrections artificially enhance turbulent Mach numbers in the near-wall region. As illustrated in Fig. 6b, the predictions of the roughness effects with the Zeman compressibility correction are in very good agreement with the experimental data for the nonblowing configuration (i.e., $F = 0$). Again, the roughness Reynolds number k_s^+ lies in the fully rough regime ($k_s^+ \approx 150$ at the end of the cone). Unfortunately, the nonblowing configuration at Mach 11 is not available in Holden's technical report [40]. Regarding the blowing configurations, both models yield very good predictions of Stanton numbers. Although the apparent roughness Reynolds number $k_s^+|_{\text{app}}$ is significantly higher than the roughness Reynolds number k_s^+, only a slight difference is visible between the two corrections. This reflects the effects of the thermal roughness correction and the compressibility correction, which mitigate the effects of the roughness/blowing correction at the high apparent roughness Reynolds number.

IV. Conclusions

RANS simulations of hypersonic turbulent flows with surface roughness and blowing effects were performed on Holden's experimental configurations [3,6] using the k–ω SST model. To reproduce blowing and roughness effects on the mean flow, different wall corrections of the turbulence model were used and compared. As the effects of turbulence compressibility grow at high Mach numbers, the Zeman and Sarkar compressibility corrections were applied to evaluate their relevance in combination with blowing or roughness wall corrections.

First, the hemispherical model at Mach 11 was considered. Compressibility corrections were not required because a subsonic region is observed downstream from the shock wave. The use of roughness corrections led to a very good agreement with experimental data and proves the efficiency of the equivalent sand grain approach for this kind of configuration. Nevertheless, particular attention must be paid to the stagnation region where the equivalent sand grain approach is not really applicable. Excellent prediction of the turbulence model were observed on the biconic configuration. The use of the Zeman correction was very satisfactory, whereas the Sarkar correction slightly underestimated the Stanton numbers over smooth walls and rough walls. In fact, for low turbulent Mach numbers, the Sarkar compressibility correction tends to overestimate the effects of the turbulence compressibility; whereas the Zeman correction remains inactive. Then, the 6 deg slender cone configuration at Mach 11 was considered. The Zeman and Sarkar compressibility corrections improved the predictions of the skin-friction coefficients and Stanton numbers by decreasing the turbulent kinetic energy in the inner region. Over rough walls, the interest in these corrections was evident because the standard k–ω SST model largely overestimated the mass and heat transfer at the wall. For this configuration, the association of compressibility corrections with a roughness correction seems adequate. Lastly, the combined effects of roughness and blowing were examined on the 10.5 deg slender cone configuration. The association of the Zeman compressibility correction and roughness or blowing/roughness wall corrections yielded good predictions of the Stanton numbers. However, compressibility corrections and roughness corrections induce an opposite effect on the turbulent kinetic energy. For this reason, their combination is delicate at high roughness Reynolds numbers.

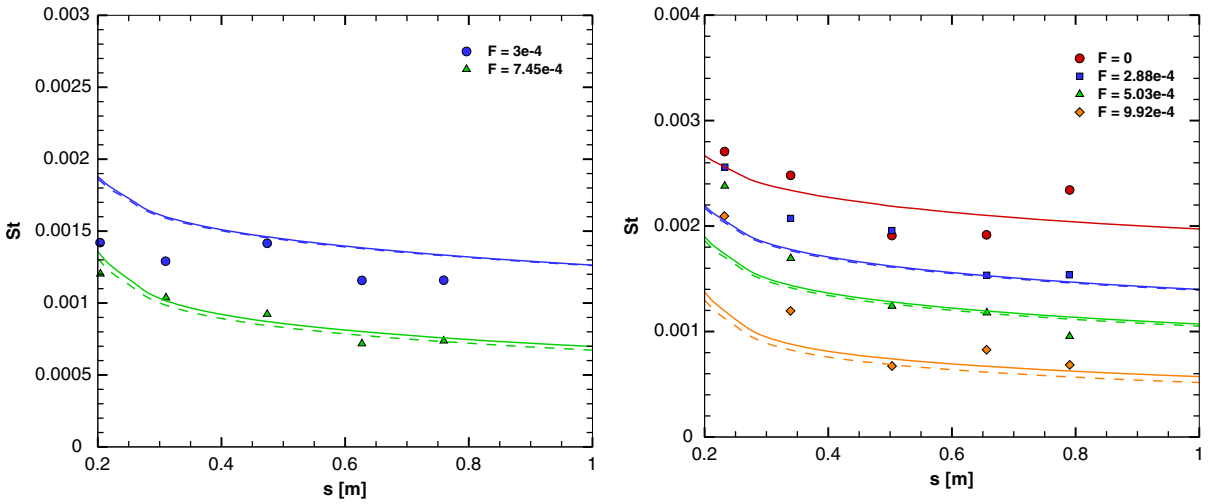

a) Stanton numbers at Mach 11

b) Stanton numbers at Mach 13

Fig. 6 Distributions of Stanton numbers St for several blowing rates F over rough walls. Full lines are results obtained using k–ω SST model with roughness/blowing correction and Zeman compressibility correction (solid), and with roughness correction and Zeman compressibility correction (dashed).

In view of the different configurations, the use of the k–ω SST model in association with blowing/roughness wall corrections and the Zeman compressibility correction seems very promising for the simulation of hypersonic boundary layers over rough walls with blowing effects.

References

[1] Voisinet, R., "Influence of Roughness and Blowing on Compressible Turbulent Boundary Layer Flow," U.S. Naval Surface Weapons Center TR-79-153', Silver Spring, MD, June 1979.

[2] Voisinet, R., "Combined Influence of Roughness and Mass Transfer on Turbulent Skin Friction at Mach 2.9," *17th Aerospace Sciences Meeting*, AIAA Paper 1979-0003, 1979. https://doi.org/10.2514/6.1979-3

[3] Holden, M., "Studies of Surface Roughness and Blowing Effects on Hypersonic Turbulent Boundary Layers over Slender Cones," *27th Aerospace Sciences Meeting*, AIAA Paper 1989-0458, 1989. https://doi.org/10.2514/6.1989-458

[4] Hill, J., and Voisinet, R., "Measurements of Surface Roughness Effects on the Heat Transfer to Slender Cones at Mach 10," *18th Aerospace Sciences Meeting*, AIAA Paper 1980-0345, 1980. https://doi.org/10.2514/6.1980-345

[5] Holden, M., "Experimental Studies of Surface Roughness, Entropy Swallowing and Boundary Layer Transition Effects on the Skin Friction and Heat Transfer Distribution in High Speed Flows," *20th Aerospace Sciences Meeting*, AIAA Paper 1982-0034, 1982. https://doi.org/10.2514/6.1982-34

[6] Holden, M., "Experimental Studies of Surface Roughness, Shape and Spacing Effects on Heat Transfer and Skin Friction in Supersonic and Hypersonic Flows," *22nd Aerospace Sciences Meeting*, AIAA Paper 1984-0016, 1984. https://doi.org/10.2514/6.1984-16

[7] Robertson, J., "Surface Resistance as a Function of the Concentration and Size of Roughness Elements," Ph.D. Thesis, State Univ. of Iowa, Iowa City, IA, Aug. 1961.

[8] Finson, M., "A Model for Rough Wall Turbulent Heating and Skin Friction," *20th Aerospace Science Meeting*, AIAA Paper 1982-0199, 1982. https://doi.org/10.2514/6.1982-199

[9] Hanson, D. R., Kinzel, M. P., and McClain, S. T., "Validation of the Discrete Element Roughness Method for Predicting Heat Transfer on Rough Surfaces," *International Journal of Heat and Mass Transfer*, Vol. 136, June 2019, pp. 1217–1232. https://doi.org/10.1016/j.ijheatmasstransfer.2019.03.062

[10] Nikuradse, J., "Strömungsgesetze in Rauhen Rohren," VDI-Forschungsheft, Vol. 361, July–Aug. 1933.

[11] Nikuradse, J., "Laws of Flows in Rough Pipes," NACA TM 1292, April 1937.

[12] Schlichting, H., "Experimental Investigation of the Problem of Surface Roughness," NACA TM 823, April 1937.

[13] Hellsten, A., and Laine, S., "Extension of the Shear-Stress Transport Turbulence Model for Rough-Wall Flows," *AIAA Journal*, Vol. 36, No. 9, 1998, pp. 1728–1729. https://doi.org/10.2514/2.7543

[14] Knopp, T., Eisfeld, B., and Calvo, J., "A New Extension for Turbulence Models to Account for Wall Roughness," *International Journal of Heat and Fluid Flow*, Vol. 30, Feb. 2009, pp. 54–65. https://doi.org/10.1016/j.ijheatfluidflow.2008.09.009

[15] Aupoix, B., and Spalart, P., "Extensions of the Spalart–Allmaras Turbulence Model to Account for Wall Roughness," *International Journal of Heat and Fluid Flows*, Vol. 24, Aug. 2003, pp. 454–462. https://doi.org/10.1016/S0142-727X(03)00043-2

[16] Aupoix, B., "Roughness Corrections for the Shear Stress Transport Model: Status and Proposals," *Journal of Fluids Engineering*, Vol. 137, Feb. 2015, Paper 021202. https://doi.org/10.1115/1.4028122

[17] Aupoix, B., "Improved Heat Transfer Predictions on Rough Surfaces," *International Journal of Heat and Fluid Flows*, Vol. 56, Dec. 2015, pp. 160–171. https://doi.org/10.1016/j.ijheatfluidflow.2015.07.007

[18] Menter, F., "Two-Equation Eddy-Viscosity Turbulence Models for Engineering Applications," *AIAA Journal*, Vol. 32, No. 8, 1994, pp. 1598–1605. https://doi.org/10.2514/3.12149

[19] Jeromin, L., "The Status of Research in Turbulent Boundary Layers with Fluid Injection," *Progress in Aerospace Sciences*, Vol. 10, 1970, pp. 65–189. https://doi.org/10.1016/0376-0421(70)90004-7

[20] Kornilov, V., "Current State and Prospects of Researches on the Control of Turbulent Boundary Layer by Air Blowing," *Progress in Aerospace Sciences*, Vol. 76, July 2015, pp. 1–23. https://doi.org/10.1016/j.paerosci.2015.05.001

[21] Stevenson, T. N., "A Law of the Wall for Turbulent Boundary Layers with Suction or Injection," College of Aeronautics, Cranfield Univ. Rept. Aero 166, 1963.

[22] Danberg, J. E., "Measurement of the Characteristics of the Compressible Turbulent Boundary Layer with Air Injection," Naval Ordnance Lab., White Oak, MD, 1959.

[23] Squire, L., "A Law of the Wall for Compressible Turbulent Boundary Layers with Air Injection," *Journal of Fluid Mechanics*, Vol. 37, No. 3, 1969, pp. 449–456. https://doi.org/10.1017/S0022112069000656

[24] Wilcox, D., "Reassessment of the Scale-Determining Equation for Advanced Turbulence Models," *AIAA Journal*, Vol. 26, No. 11, 1988, pp. 1299–1310. https://doi.org/10.2514/3.10041

[25] Marchenay, Y., Chedevergne, F., and Olazabal Loumé, M., "Modeling of Combined Effects of Surface Roughness and Blowing for Reynolds-Averaged Navier–Stokes Turbulence Models," *Physics of Fluids*, Vol. 33, No. 4, 2021, Paper 045116. https://doi.org/10.1063/5.0042960

[26] Sarkar, S., "The Pressure-Dilatation Correlation in Compressible Flows," *Physics of Fluids A*, Vol. 4, No. 12, 1992, pp. 2674–2682. https://doi.org/10.1063/1.858454

[27] Zeman, O., "Dilatation Dissipation: The Concept and Application in Modeling Compressible Mixing Layers," *Physics of Fluids A*, Vol. 2, No. 2, 1990, pp. 178–188. https://doi.org/10.1063/1.857767

[28] Rumsey, C., "Compressibility Considerations for k–ω Turbulence Models in Hypersonic Boundary Layer Applications," NASA TM 2009-215705, 2009. https://doi.org/10.2514/1.45350

[29] Zhu, Z., Zhang, X., Wang, X., and Zhang, L., "Analysis of Compressibility Corrections for Turbulence Models in Hypersonic Boundary-Layer Applications," *Journal of Spacecraft and Rockets*, Vol. 57, No. 2, 2020, pp. 364–372. https://doi.org/10.2514/1.A34544

[30] Sarkar, S., Erlebacher, G., Hussaini, M. Y., and Kreiss, H. O., "The Analysis and Modelling of Dilatational Terms in Compressible Turbulence," *Journal of Fluid Mechanics*, Vol. 227, June 1991, pp. 473–493. https://doi.org/10.1017/S0022112091000204

[31] Zeman, O., "A New Model for Super/Hypersonic Turbulent Boundary Layers," *31st Aerospace Sciences Meeting*, AIAA Paper 1993-0897, 1993. https://doi.org/10.2514/6.1993-897

[32] Wilcox, D. C., "Dilatation-Dissipation Corrections for Advanced Turbulence Models," *AIAA Journal*, Vol. 30, No. 11, 1992, pp. 2639–2646. https://doi.org/10.2514/3.11279

[33] McClain, S., Collins, S., Hodge, B., and Bons, J., "The Importance of the Mean Elevation in Predicting Skin Friction for Flow over Closely Packed Surface Roughness," *Journal of Fluids Engineering*, Vol. 128, Oct. 2005, pp. 579–586. https://doi.org/10.1115/1.2175164

[34] Andersen, P., Kays, W., and Moffat, R., "Experimental Results for the Transpired Turbulent Boundary Layer in an Adverse Pressure Gradient," *Journal of Fluid Mechanics*, Vol. 69, No. 2, 1975, pp. 353–375. https://doi.org/10.1017/S0022112075001474

[35] Healzer, J., Kays, W., and Moffat, R., "The Turbulent Boundary Layer on a Porous, Rough Plate: Experimental Heat transfer with Uniform Blowing," *Thermophysics and Heat Transfer Conference*, AIAA Paper 1974-0680, 1974. https://doi.org/10.2514/6.1974-680

[36] Pimenta, M., Moffat, R., and Kays, W., "The Structure of a Boundary Layer on a Rough Wall with Blowing and Heat Transfer," *Journal of Heat Transfer*, Vol. 101, May 1979, pp. 193–198. https://doi.org/10.1115/1.3450945

[37] Dirling, R., Jr., "A Method for Computing Rough Wall Heat Transfer Rates on Reentry Nosetips," *AIAA 8th Thermophysics Conference*, AIAA Paper 1973-0763, 1973. https://doi.org/10.2514/6.1973-763

[38] Sigal, A., and Danberg, J., "New Correlation of Roughness Density Effect on the Turbulent Boundary Layer," *AIAA Journal*, Vol. 28, No. 3, 1990, pp. 554–556. https://doi.org/10.2514/3.10427

[39] van Rij, J., Belnap, B., and Ligrani, P., "Analysis and Experiments on Three-Dimensional, Irregular Surface Roughness," *Journal of Fluid Engineering*, Vol. 124, Aug. 2002, pp. 671–677. https://doi.org/10.1115/1.1486222

[40] Holden, M., "Studies of Boundary Layer Transition and Surface Roughness Effects in Hypersonic Flows," U.S. Air Force Office of Scientific Research AFOSR-TR-84-0251, Bolling AFB, D.C., Oct. 1983.

[41] Holden, M., Mundy, E., and Wadhams, T., "A Review of Experimental Studies of Surface Roughness and Blowing on the Heat Transfer and Skin Friction to Nosetips and Slender Cones in High Mach Numbers Flows," *40th Thermophysics Conference*, AIAA Paper 2008-3907, 2008.
https://doi.org/10.2514/6.2008-3907

[42] Hansen, C. F., *Thermodynamic and Transport Properties of High-Temperature Air*, Advisory Group for Aeronautical Research and Development, Paris, France, 1959.

[43] Holden, M., "An Experimental Study of Transpiration Cooling on the Distribution of Heat Transfer and Skin Friction to a Sharp Slender Cone at Mach 11 and 13," *28th Aerospace Sciences Meeting*, AIAA Paper 1990-0308, 1990.
https://doi.org/10.2514/6.1990-308

[44] Holden, M., van Osdol, J., and Rodriguez, K., "An Experimental Study of the Effects of Injectant Properties on the Aerothermal Characteristics of Transpiration-Cooled Coned in Hypersonic Flows," *21st Fluid Dynamics, Plasma Dynamics and Laser Conference*, AIAA Paper 1990-1487, 1990.
https://doi.org/10.2514/6.1990-1487

[45] Holden, M., Mundy, E., and MacLean, M., "Heat Transfer Measurements to Examine Surface Roughness and Blowing Effects in Hypersonic Flows," *40th Aerospace Sciences Meeting*, AIAA Paper 2011-0760, 2011.
https://doi.org/10.2514/6.2011-760

S. Silton
Associate Editor